Journal of Orthopaedic Translation 50 (2025) 1–13

Contents lists available at ScienceDirect

Journal of Orthopaedic Translation

journal homepage: www.journals.elsevier.com/journal-of-orthopaedic-translation

Original Article

Paeonol inhibits ACSL4 to protect chondrocytes from ferroptosis and ameliorates osteoarthritis progression

Siyang Cao [a,b,c,2], Yihao Wei [a,b,d,e,2], Ao Xiong [a,b,c,2], Yaohang Yue [a,b,c], Jun Yang [f], Deli Wang [a,b,c], Xiyu Liu [h], Hui Zeng [a,b,g,1,*], Dongquan Shi [h,**,1], Ye Li [d,***,1]

[a] National & Local Joint Engineering Research Centre of Orthopaedic Biomaterials, Peking University Shenzhen Hospital, Shenzhen, Guangdong, China
[b] Shenzhen Key Laboratory of Orthopaedic Diseases and Biomaterials Research, Peking University Shenzhen Hospital, Shenzhen, Guangdong, China
[c] Department of Bone & Joint Surgery, Peking University Shenzhen Hospital, Shenzhen, Guangdong, China
[d] Department of Rehabilitation Science, The Hong Kong Polytechnic University, Hong Kong Special Administrative Region, China
[e] Faculty of Pharmaceutical Sciences, Shenzhen Institute of Advanced Technology, Chinese Academy of Sciences (CAS), Shenzhen, Guangdong, China
[f] Department of Radiology, Peking University Shenzhen Hospital, Shenzhen, Guangdong, China
[g] Department of Orthopedics, Shenzhen Second People's Hospital, The First Affiliated Hospital of Shenzhen University, Shenzhen, Guangdong, China
[h] Division of Sports Medicine and Adult Reconstructive Surgery, Department of Orthopaedic Surgery, Nanjing Drum Tower Hospital, Affiliated Hospital of Medical School, Nanjing University, Nanjing, Jiangsu, China

ARTICLE INFO

Keywords:
ACSL4
Chondrocytes
Ferroptosis
Osteoarthritis
Paeonol

ABSTRACT

Background: Discovering an inhibitor for acyl-CoA synthetase long-chain family member 4 (ACSL4), a protein that triggers cell injury via ferroptosis, presents potential to minimize cellular damage. This study investigates paeonol (PAE), a traditional Chinese herbal medicine, as an ACSL4 inhibitor to prevent chondrocyte ferroptosis and protect against osteoarthritis (OA).

Methods: We conducted *in vitro* experiments using mouse chondrocytes treated with PAE to mitigate ferroptosis induced by Interleukin-1 Beta (IL-1β) or ferric ammonium citrate (FAC), examining intracellular ferroptotic indicators, cartilage catabolic markers, and ferroptosis regulatory proteins. A mouse OA model was created via destabilized medial meniscus (DMM), followed by intra-articular PAE injections. After 8 weeks, micro-computed tomography and histological assessments evaluated PAE's protective and anti-ferroptotic effects in the OA model.

Results: In vitro results showed PAE significantly reduced IL-1β/FAC-induced damage by targeting ACSL4, including cell apoptosis, inflammatory responses, extracellular matrix degradation, and ferroptotic markers (oxidative stress, lipid peroxidation, and iron buildup). It also restored the expression of ferroptotic suppressors and mitigated mitochondrial damage. Additionally, PAE increased cartilage anabolic marker expression while reducing cartilage catabolic marker expression. Molecular docking, cellular thermal shift assay, and drug affinity responsive target stability analysis verified the binding interaction between PAE and ACSL4. Furthermore, the role of PAE in chondrocytes was further verified through ACSL4 knockdown and overexpression. *In vivo*, mice with OA showed increased cartilage degradation and ferroptosis, while intra-articular PAE injection alleviated these pathological changes.

Conclusion: PAE significantly protects chondrocytes from ferroptosis induced by IL-1β/FAC in primary mouse chondrocytes and DMM surgery-induced OA mice through ACSL4 inhibition.

The translational potential of this article: These findings highlight the potential of targeting ACSL4 in chondrocytes as a treatment strategy for OA, positioning PAE as a promising drug candidate.

* Corresponding author. National & Local Joint Engineering Research Centre of Orthopaedic Biomaterials, Peking University Shenzhen Hospital, Shenzhen, Guangdong, China.
** Corresponding author.
*** Corresponding author.
E-mail addresses: zenghui@pkuszh.com (H. Zeng), shidongquan@nju.edu.cn (D. Shi), yejulie.li@polyu.edu.hk (Y. Li).
[1] Hui Zeng, Dongguan Shi, and Ye Li contributed equally to this work and share last authorship.
[2] Siyang Cao, Yihao Wei, and Ao Xiong contributed equally to this work and share first authorship.

https://doi.org/10.1016/j.jot.2024.10.005
Received 25 July 2024; Received in revised form 9 October 2024; Accepted 19 October 2024
Available online 24 November 2024

1. Introduction

Osteoarthritis (OA), affecting about 7 % of the global population, is the most prevalent type of arthritis [1]. The incidence of OA is rising with the aging population and obesity epidemic, leading to significant health and economic burdens [2]. Despite long-term recognition, effective therapies to alter OA progression are lacking primarily because of the intricate mechanisms involved in its pathogenesis. The Food and Drug Administration of the United States categorizes OA as a "serious condition with significant medical needs that remain unfulfilled" [3]. Cartilage degeneration is the primary pathogenesis of OA progression, and various chondrocyte injuries directly accelerate this process [4]. Different forms of chondrocyte death, including ferroptosis, have been recognized in the degeneration of cartilage [5]. Recent studies show that ferroptosis promotes OA progression by inducing chondrocyte dysfunction and injury [6,7]. Thus, inhibiting chondrocyte ferroptosis has emerged as an effective strategy to delay OA progression [7].

Acyl-CoA synthetase long-chain family member 4 (ACSL4), a key marker of ferroptosis, catalyzes the biosynthesis of lipids with polyunsaturated fatty acids [8]. It esterifies arachidonic and adrenic acids to phosphatidylethanolamine, promoting lipid peroxide accumulation and ferroptosis [9]. Inhibiting ACSL4 is an effective method to protect cells from ferroptosis [10], which is evident in OA progression. Xu et al. illustrated that the upregulation of ACSL4 expression in the affected cartilage region exceeded that in the unaffected area, intensifying as human OA progressed [11]. In preclinical OA models, ACSL4 protein levels were increased in Interleukin-1 Beta (IL-1β)-stimulated chondrocytes [12,13]. Knockdown of ACSL4 mitigated the ferroptotic effects induced by IL-1β on chondrocytes [13]. The results indicate that focusing on ACSL4 may represent a viable treatment strategy for addressing OA.

Extensive clinical knowledge has been amassed over thousands of years in Traditional Chinese Medicine (TCM), making a significant impact on human health [14]. Targeting ferroptosis unveils a new epoch for TCM [15]. Paeonol (PAE, 2′-hydroxy-4′-methoxyacetophenone) is a small molecule phenolic compound that could be isolated from several TCMs (e.g., peony bark, paeonia rubra, and Xu Changqing) [16]. With the modernization of TCM, PAE has gained attention for its broad pharmacological effects, including anti-atherosclerosis, antiplatelet aggregation, anti-oxidation, and anti-inflammatory properties [17]. It has been discovered that PAE can prevent lipid peroxidation and ferroptosis in neurons, cardiomyocytes, and endometrial epithelial cells by inhibiting the activity of ACSL4 [18–20]. However, the impact of PAE on ferroptosis in osteoarthritic chondrocytes remains unclear, suggesting a potential therapeutic approach for OA [21].

This research employed IL-1β to model inflammation and utilized ferric ammonium citrate (FAC) to represent iron overload *in vitro*. An *in vivo* model of OA was established using a surgically induced destabilization of the medial meniscus (DMM) in mice. We seek to uncover how PAE contributes to the prevention of chondrocyte damage by focusing on ACSL4 to inhibit ferroptosis, which in turn helps to slow down the progression of OA.

2. Methods & materials

Detailed methods and materials are provided in the Results Section and Supplementary File.

2.1. Chemical & biological reagents

The study utilized the following materials and reagents: complete DMEM: Nutrient Mixture F12 medium (DMEM/F12) (PM150310B, Procell, Wuhan, China), 0.25 % trypsin–EDTA (G4001, Servicebio), Cell Counting Kit-8 (C0037, Beyotime), PAE (R011869, Rhawn), FAC (R017760, Rhawn), Pronase (10165921001, Roche, Switzerland), Recombinant Mouse IL-1β (211-11 B, PeproTech), Annexin V-FITC/Propidium Iodide (PI) Apoptosis Detection Kit (AD10, Dojindo), Calcein-AM/PI Double Staining Kit (C542, Dojindo), BeyoClick™ EdU Cell Proliferation Kit with Alexa Fluor 555 (C0075S, Beyotime), FerroOrange (F374, Dojindo), Prussian Blue Iron (PBI) Stain Kit for Cell (G1426, Solarbio), Reactive Oxygen Species (ROS) Assay Kit (S0033S, Beyotime), mtSOX Deep Red (MT14, Dojindo), GSH and GSSG Assay Kit (S0053, Beyotime), Malondialdehyde (MDA) Assay Kit (S0131S, Beyotime), Ferrous Ion Content Assay Kit (BC5410, Solarbio), Glutamate Content Assay Kit (BC1585, Solarbio), Glutamine Content Assay Kit (G0429W, Geruisi), Superoxide Dismutase (SOD) Activity Assay Kit (BC5165, Solarbio), Mitochondrial Membrane Potential (ΔΨm) Assay Kit with Rhodamine 123 (C2008S, Beyotime), Mito-Tracker Green (MTG) (C1048, Beyotime), Toluidine Blue (TB) Cartilage Stain Solution (G1032, Servicebio), Saffron-O and Fast Green (SOFG) Stain Solution (G1053, Servicebio), Hematoxylin-Eosin (H&E) Stain Solution (G1005, Servicebio).

The commercial enzyme-linked immunosorbent assay (ELISA) kits used were: Mouse 4-Hydroxynonenal (4-HNE) ELISA Kit (EM1583, FineTest), Mouse Nitric Oxide Synthase 2 (iNOS) ELISA Kit (EM0272, FineTest), Mouse Phospholipid Hydroperoxide Glutathione peroxidase (GPx4) ELISA Kit (EM1964, FineTest), Mouse Interleukin-6 (IL-6) ELISA Kit (RK00008, ABclonal), Mouse Cyclooxygenase-2 (COX-2) ELISA Kit (RK03142, ABclonal), and Mouse Tumor Necrosis Factor-alpha (TNF-α) ELISA Kit (RK00027, ABclonal).

The commercial antibodies used were: MMP3 (FNab05244, FineTest), ADAMTS5 (bs-3573R, Bioss), COL2A1 (FNab01837, FineTest), SOX9 (FNab10948, FineTest), Aggrecan (A11691, ABclonal), LPCAT3 (A17604, ABclonal), MMP13 (FNab05235, FineTest), ACSL4 (A20414, ABclonal), SLC7A11 (FNab10533, FineTest), GPx4 (FNab03622, FineTest), COX-2 (A1253, ABclonal), 4-HNE (bs-6313R, Bioss), GAPDH (5174S, Cell Signaling Technology), FITC Goat Anti-Rabbit IgG (H + L) (AS011, ABclonal), Anti-rabbit IgG (H + L), F(ab')2 Fragment (Alexa Fluor® 555 Conjugate) (4413S, Cell Signaling Technology), and HRP Goat Anti-Rabbit IgG (H + L) (AS014, ABclonal).

2.2. Statistical analysis

Data were compiled and independently analyzed by two authors. All analyses were conducted with GraphPad Prism 9.5 (GraphPad Software, San Diego, USA). Quantitative data represent the results of at least three independent experiments, with only data from a representative experiment presented. Student's *t*-tests were utilized for pairwise comparisons, while one-way analysis of variance (ANOVA) was employed for comparisons among multiple groups. The data is presented as mean ± standard deviation (SD). Two-tailed *P* values were calculated with statistical significance defined as $P < 0.05$, denoted as 'ns' for no statistical difference, and indicated as $^{*}P < 0.05$, $^{**}P < 0.01$, $^{***}P < 0.001$. All experiments and images shown are representative.

3. Results

3.1. PAE protects chondrocytes from IL-1β/FAC-induced proliferation inhibition and cell death

Fig. 1A illustrates the chemical structure of PAE. After 24 h, the cytotoxicity of varying PAE concentrations on chondrocytes was assessed (Fig. 1B). PAE treatments at concentrations of 50, 100, and 200 μM for 24 h significantly reduced chondrocyte viability ($P < 0.05$), whereas concentrations between 0 and 25 μM showed no significant cytotoxicity. Based on these findings, 25 μM PAE was chosen for subsequent *in vitro* experiments. The 5-Ethynyl-2′-Deoxyuridine (EdU) assay (Fig. 1C and E) confirmed that IL-1β and FAC significantly inhibited chondrocyte proliferation. However, PAE partially restored the proliferation of cells inhibited by IL-1β/FAC ($P < 0.05$), indicating its protective effect on chondrocytes. This result was further validated by Calcein-AM/PI double staining ($P < 0.05$) (Fig. 1D and F). These

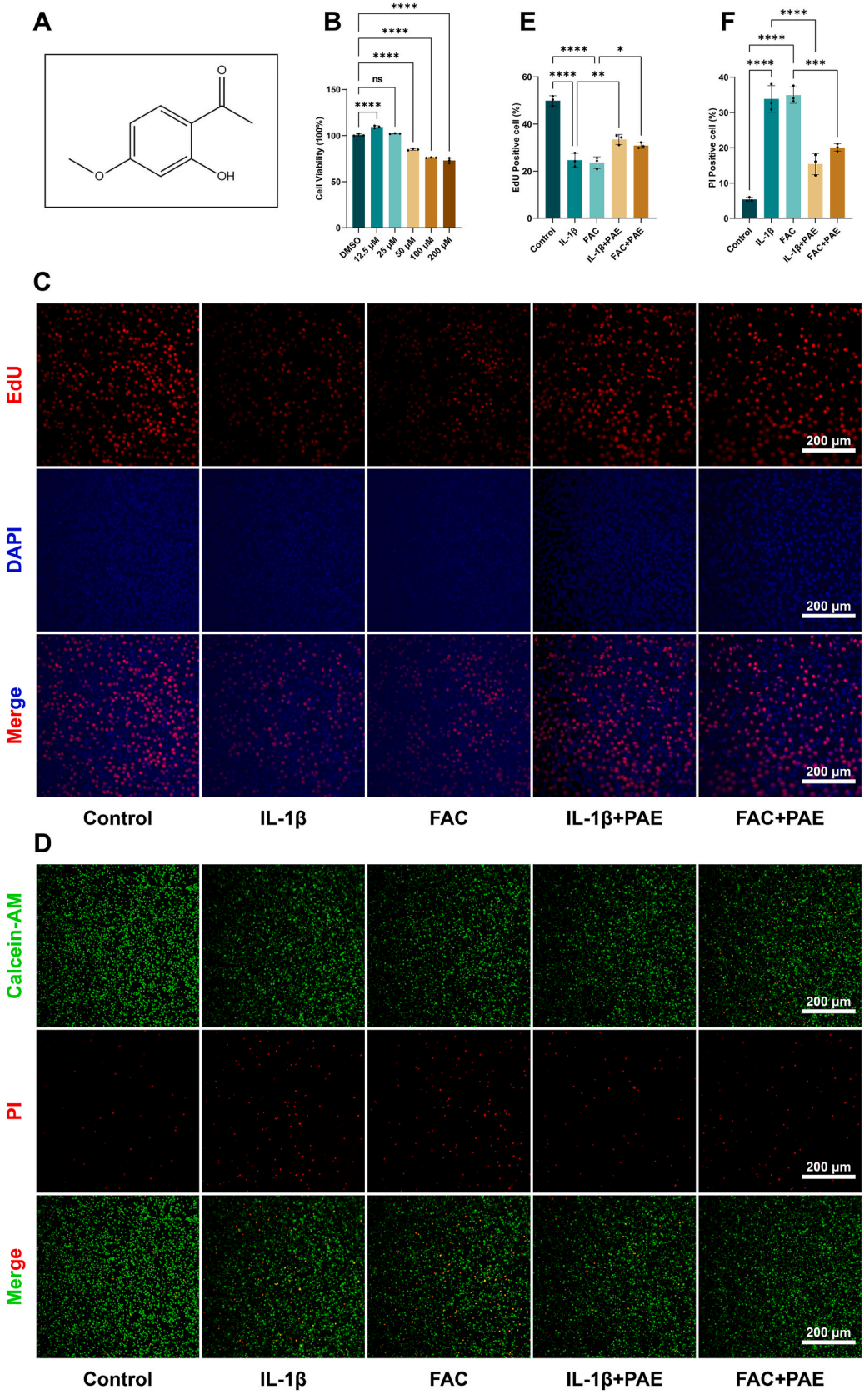

(caption on next page)

Fig. 1. PAE protects chondrocytes from IL-1β/FAC-induced proliferation inhibition and cell death: (A) PAE structural formula (molecular formula: $C_9H_{10}O_3$; molecular weight: 166.17). (B) Chondrocytes were treated with PAE at concentrations of 0, 12.5, 25, 50, 100, and 200 μM for 24 h (n = 3 per group). (C) Cell proliferation was determined by EdU staining (scale bar = 200 μm. (D) Calcein-AM/PI double staining (scale bar = 200 μm). (E) Semi-quantitative analysis of EdU staining fluorescence intensity (n = 3 per group). (F) Semi-quantitative analysis of PI staining assay results (n = 3 per group). Two-tailed *P* values were calculated with statistical significance defined as $P < 0.05$, denoted as 'ns' for no statistical difference, and indicated as $^*P < 0.05$, $^{**}P < 0.01$, $^{***}P < 0.001$. All experiments and images shown are representative.

findings demonstrate that PAE protects chondrocytes from IL-1β/FAC-induced proliferation inhibition and cell death.

3.2. PAE reduces IL-1β/FAC-induced inflammation, extracellular matrix (ECM) degradation, oxidative stress, and apoptosis

IL-1β is commonly used to induce inflammation in chondrocytes as an *in vitro* model for OA, while FAC is used to create an iron overload cell model [6]. In our research, there was a significant increase in the expression levels of proinflammatory cytokines (including COX-2, iNOS, IL-6, and TNF-α) in both the IL-1β and FAC model groups. Conversely, PAE significantly lowered these cytokines ($P < 0.05$) (Fig. 2Ã2F). Matrix metallopeptidase 3 (MMP3), matrix metallopeptidase 13 (MMP13), and ADAM metallopeptidase with thrombospondin type 1 motif 5 (ADAMTS5) are essential enzymes degrading the matrix involved in OA cartilage destruction [22,23]. Western Blot results indicated that IL-1β and FAC promoted cartilage catabolism, while PAE significantly suppressed this effect ($P < 0.05$) (Fig. 2E and F). Collagen Type II Alpha 1 Chain (COL2A1), SRY-Box Transcription Factor 9 (SOX9), and Aggrecan are well-known chondrogenic markers [24]. Western Blot results showed that IL-1β and FAC reduced cartilage ECM anabolism, while PAE significantly reversed this effect (Supplementary Fig. S1). Additionally, the DCFH-DA fluorescent probe was utilized to detect intracellular ROS levels. IL-1β/FAC induced an increase in ROS in chondrocytes, which was significantly reduced after PAE treatment (Fig. 2G and H) ($P < 0.05$). Annexin V-FITC/PI staining was employed to assess PAE's protective effect against IL-1β/FAC-induced apoptosis in chondrocytes. Apoptosis was significantly higher in IL-1β and FAC-treated groups compared to the control group ($P < 0.05$) (Fig. 2I and J). Conversely, PAE treatment mitigated the apoptotic impact of inflammation and iron overload in chondrocytes. These results demonstrate that PAE alleviates IL-1β/FAC-induced inflammation, ECM degradation, oxidative stress, and apoptosis in chondrocytes.

3.3. PAE mitigates IL-1β/FAC-induced ferroptosis in chondrocytes

Several markers, including GPx4 and solute carrier family 7 member 11 (SLC7A11), show decreased expression during ferroptosis, while ACSL4 undergoes an increase in expression. These changes in marker expression signify ferroptosis [25]. Under conditions of inflammation or iron overload, GPx4 and SLC7A11 protein expression significantly decreased, while ACSL4 and its downstream signal factor (lysophosphatidylcholine acyltransferase 3 (LPCAT3)) expression increased substantially (Fig. 3A, B, 3F, and Supplementary Fig. S1) ($P < 0.05$). These findings suggest that IL-1β and FAC induce ferroptosis in chondrocytes. PAE significantly inhibited ACSL4 and LPCAT3 expression, while enhancing GPx4 and SLC7A11 expression in chondrocytes, highlighting its anti-ferroptotic efficacy (Fig. 3A, B, 3F and Supplementary Fig. S1) ($P < 0.05$). MDA and 4-HNE, primary biomarkers for lipid peroxidation and ferroptosis, are implicated in various pathological processes associated with OA development [26]. IL-1β/FAC exposure elevated MDA and 4-HNE levels in chondrocytes, an effect significantly reduced by PAE treatment (Fig. 3C and E) ($P < 0.05$).

Given the involvement of cellular iron accumulation in ferroptosis, this study analyzed ferrous and ferric ion levels [27]. The ferrous ion content assay kit showed that Fe^{2+} concentration increased in IL-1β/FAC-treated cells, while PAE treatment significantly reduced Fe^{2+} levels (Fig. 3D) ($P < 0.05$). Chondrocytes were also stained with FerroOrange, which selectively reacts with Fe^{2+} rather than Fe^{3+}. FerroOrange signal intensity increased significantly with Fe^{2+} concentration in IL-1β/FAC-treated cells, while PAE treatment significantly reduced Fe^{2+} levels (Fig. 3J and K) ($P < 0.05$). Intracellular iron deposits were detected by PBI staining, which showed increased iron content after IL-1β/FAC treatment. PAE-treated chondrocytes exhibited some resistance to intracellular iron accumulation (Fig. 3L).

SOD activity, assessed in various treatment groups, was inhibited in IL-1β/FAC-treated chondrocytes, while PAE partially restored SOD activity (Fig. 3G) ($P < 0.05$). Reduced glutathione (GSH), oxidized glutathione (GSSG), and the GSH/GSSG ratio were also assessed. The IL-1β and FAC group displayed a significant reduction in both GSH and the GSH/GSSG ratio, while GSSG levels were notably elevated when contrasted with the control group (Fig. 3H) ($P < 0.05$). In rescue experiments, PAE reversed the decline in GSH and the GSH/GSSG ratio while increasing GSSG levels ($P < 0.05$). Considering that glutamate and glutamine contribute to the production of GSH and nicotinamide adenine dinucleotide phosphate, intracellular ROS levels were inferred by measuring glutamate and glutamine concentrations. Lower glutamine levels correspond to higher ROS levels, while higher glutamate levels indicate lower ROS levels [28]. Analysis of glutamine and glutamate content in each experimental group showed a consistent trend: IL-1β and FAC increased intracellular glutamate levels while decreasing glutamine levels in chondrocytes (Fig. 3I) ($P < 0.05$). PAE treatment reversed these effects (Fig. 3I) ($P < 0.05$). These results demonstrate the ability of PAE to alleviate IL-1β/FAC-induced ferroptosis in chondrocytes.

3.4. PAE alleviates IL-1β/FAC-induced mitochondrial injury

Lipid peroxidation damages mitochondria during ferroptosis [9,29]. We assessed intracellular oxidative stress levels within mitochondria using the mtSOX Deep Red probe. IL-1β/FAC-induced oxidative stress increased mitochondrial ROS release, evidenced by heightened mtSOX Deep Red intensity (Fig. 4A and B) ($P < 0.05$). PAE treatment decreased mitochondrial ROS levels in chondrocytes (Fig. 4A and B) ($P < 0.05$). Ferroptosis is associated with abnormal ΔΨm [30]. IL-1β/FAC treatment impaired ΔΨm, indicated by reduced fluorescence intensity following Rhodamine 123 staining, which was partially restored by PAE administration (Fig. 4C and D) ($P < 0.05$). We employed MTG kits to assess mitochondrial mass. Chondrocytes treated with IL-1β/FAC showed reduced mitochondrial mass (Fig. 5E and F) ($P < 0.05$). PAE mitigated the IL-1β/FAC-induced loss of organelle mass (Fig. 5E and F) ($P < 0.05$).

Ferroptosis is characterized by cellular structural alterations such as mitochondrial atrophy and changes in mitochondrial cristae, setting it apart from other types of cell death [25]. To further investigate IL-1β/FAC impact on mitochondria *in vitro* and evaluate PAE's potential protective effects, we employed transmission electron microscopy (TEM) to examine mitochondrial ultrastructure. Fig. 4G shows IL-1β/FAC induced mitochondrial structure alterations indicative of ferroptosis, which were significantly attenuated by PAE treatment. These findings suggest PAE can ameliorate mitochondrial damage caused by lipid peroxidation, highlighting its potential as an anti-ferroptotic agent.

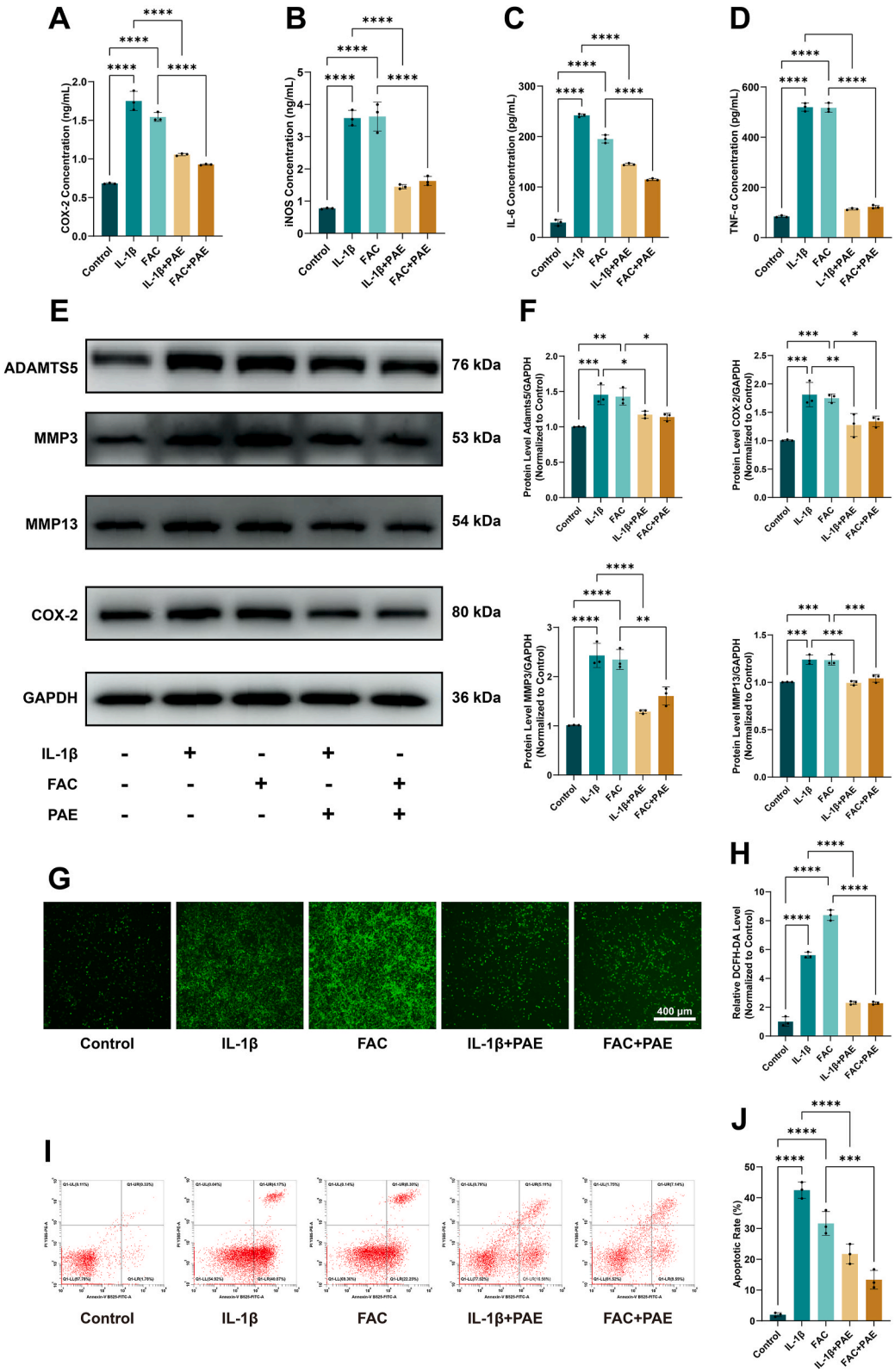

Fig. 2. PAE reduces IL-1β/FAC-induced inflammation, ECM degradation, oxidative stress, and apoptosis: (A∼D) ELISA used to detect proinflammatory cytokines (COX-2, iNOS, IL-6, TNF-α) (n = 3 per group). (E) Western Blot analysis of ADAMTS5, MMP3, MMP13, and COX-2 protein levels. (F) Quantification of protein expression by band densitometry, normalized to GAPDH (n = 3 per group). (G) Intracellular ROS detected using DCFH-DA and visualized with fluorescence microscopy (scale bar = 400 μm). (H) Quantification of DCFH-DA fluorescence intensity (n = 3 per group). (I) Apoptosis assessed by Annexin V-FITC/PI staining. (J) Quantitative analysis of apoptosis rate (n = 3 per group). Two-tailed *P* values were calculated with statistical significance defined as $P < 0.05$, denoted as 'ns' for no statistical difference, and indicated as $^{*}P < 0.05$, $^{**}P < 0.01$, $^{***}P < 0.001$. All experiments and images shown are representative.

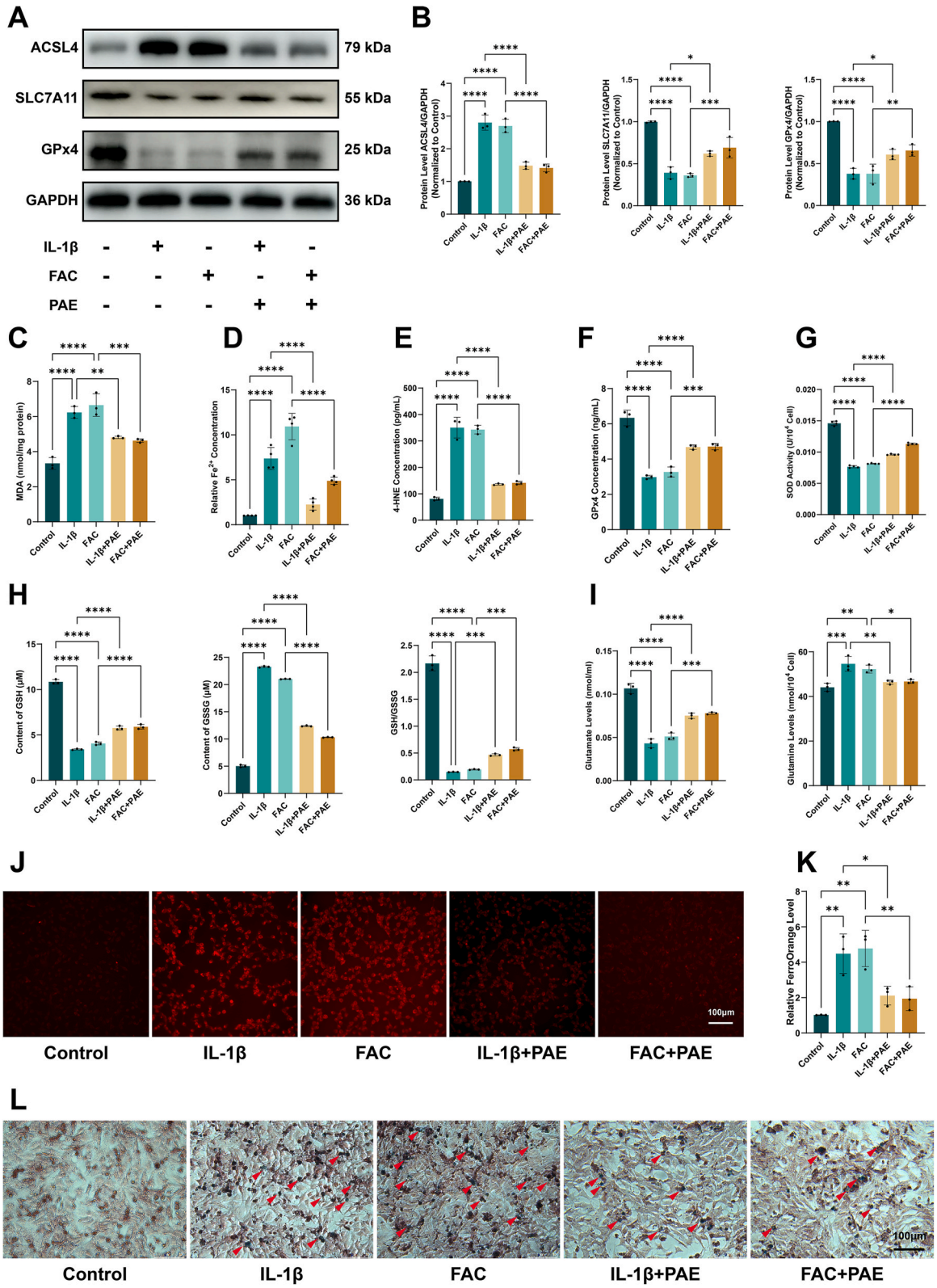

Fig. 3. PAE mitigates IL-1β/FAC-induced ferroptosis in chondrocytes: (A) Western Blot analysis of ACSL4, SLC7A11, and GPx4 protein levels. (B) Quantification of protein expression by band densitometry, normalized to GAPDH (n = 3 per group). (C) MDA content measured using a lipid peroxidation MDA assay kit (n = 3 per group). (D) Fe^{2+} levels in chondrocytes detected using a Fe^{2+} content assay kit (n = 4 per group). (E) 4-HNE levels in chondrocytes determined by ELISA (n = 3 per group). (F) GPx4 protein levels detected by ELISA (n = 3 per group). (G) Measurement of intracellular SOD activity (n = 4 per group). (H) Intracellular GSH, GSSG content, and GSH/GSSG (glutathione redox ratio) (n = 4 per group). (I) Glutamate and glutamine levels (n = 3 per group). (J) Intracellular Fe^{2+} visualized by FerroOrange using fluorescence microscopy (scale bar = 100 μm). (K) Quantification of FerroOrange fluorescence intensity (n = 3 per group). (L) Prussian blue staining of chondrocytes with red arrows indicating iron deposition (scale bar = 100 μm). Two-tailed *P* values were calculated with statistical significance defined as $P < 0.05$, denoted as 'ns' for no statistical difference, and indicated as $^{*}P < 0.05$, $^{**}P < 0.01$, $^{***}P < 0.001$. All experiments and images shown are representative. (For interpretation of the references to colour in this figure legend, the reader is referred to the Web version of this article.)

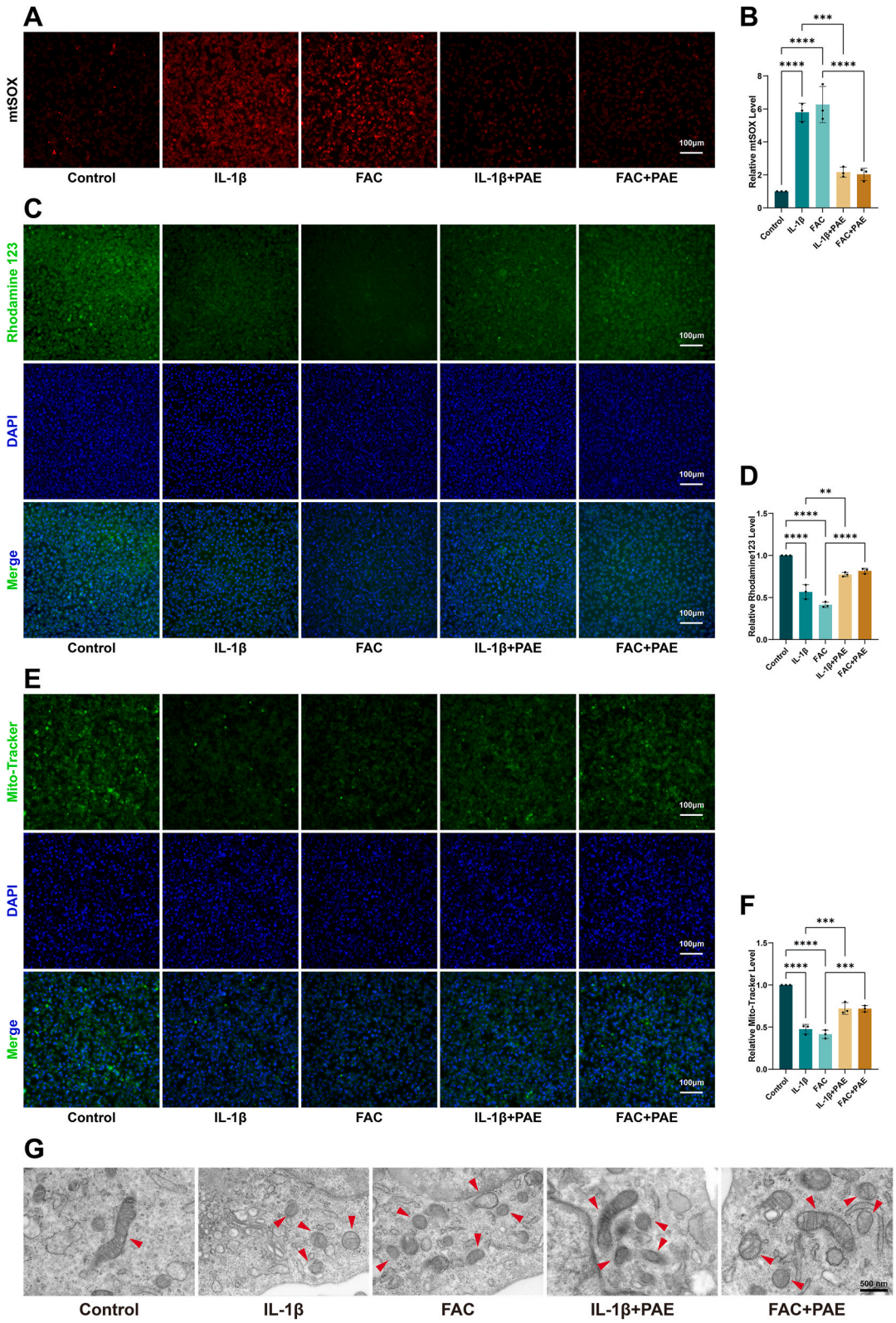

Fig. 4. PAE alleviates IL-1β/FAC-induced mitochondrial injury: (A) Mitochondrial oxidative stress levels assessed by mtSOX Deep Red and visualized via fluorescence microscopy (scale bar = 100 μm). (B) Mitochondrial membrane potential changes detected using Rhodamine 123 (scale bar = 100 μm). (C) Mitochondrial mass evaluated by Mito-Tracker Green staining (scale bar = 100 μm). (D) Quantification of mtSOX Deep Red fluorescence intensity (n = 3 per group). (E) Quantification of Rhodamine 123 fluorescence intensity (n = 3 per group. (F) Quantification of Mito-Tracker Green fluorescence intensity (n = 3 per group). (G) Mitochondria in chondrocytes visualized by TEM, with red arrows indicating mitochondria (scale bar = 500 nm). Two-tailed *P* values were calculated with statistical significance defined as $P < 0.05$, denoted as 'ns' for no statistical difference, and indicated as $^{*}P < 0.05$, $^{**}P < 0.01$, $^{***}P < 0.001$. All experiments and images shown are representative. (For interpretation of the references to colour in this figure legend, the reader is referred to the Web version of this article.)

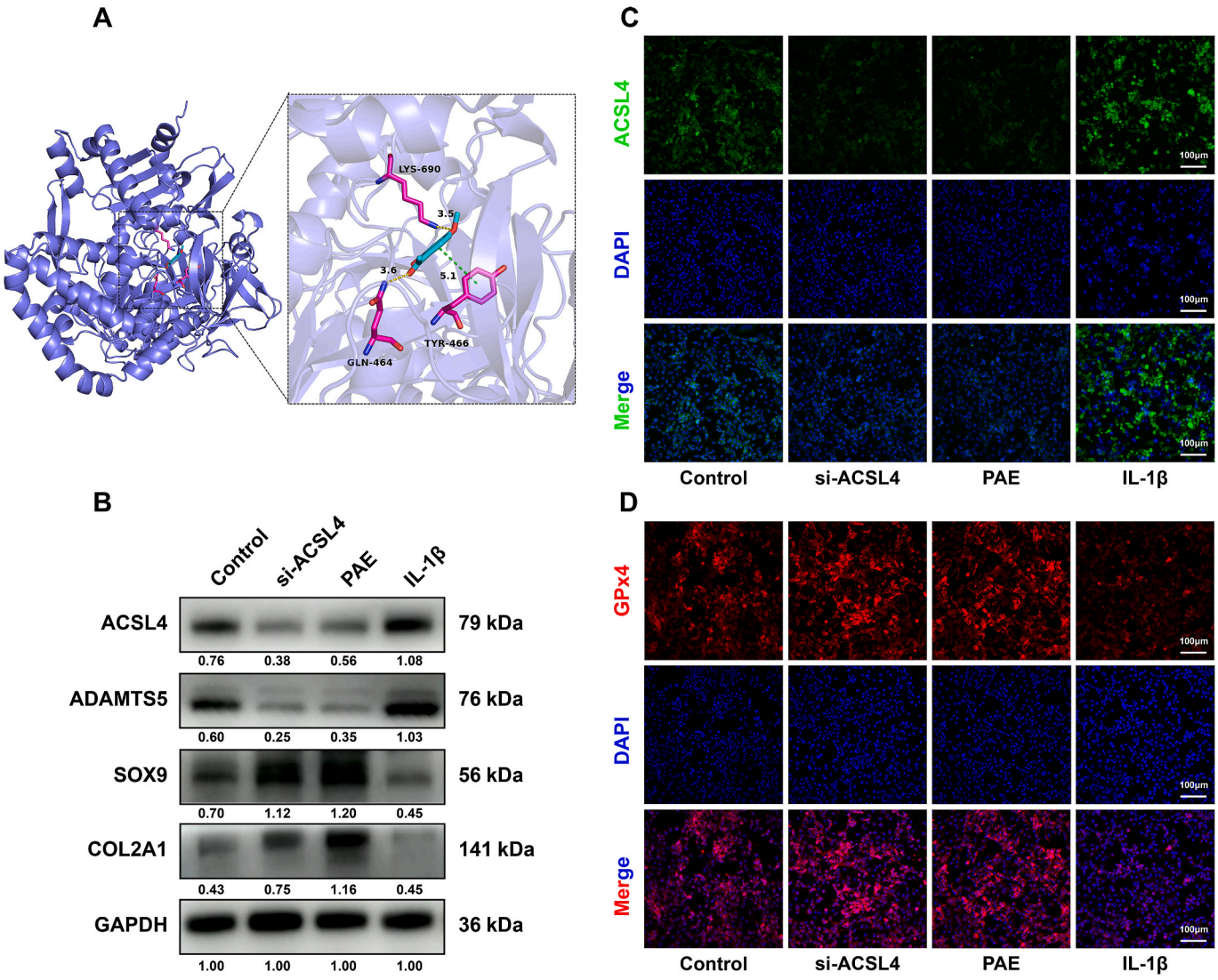

Fig. 5. PAE exhibits a comparable chondrocyte-protective and anti-ferroptotic effect to ACSL4 knockdown in chondrocytes: (A) Molecular docking of PAE with ACSL4. ACSL4 protein is depicted as a slate cartoon model, the ligand as a cyan stick, and binding sites as magenta sticks. Nonpolar hydrogen atoms are omitted. Hydrogen bonds, ionic interactions, and hydrophobic interactions are represented by yellow, magenta, and green dashed lines, respectively. (B) Protein expression levels of ACSL4, ADAMTS5, SOX9, and COL2A1 were detected by Western Blot. (C, D) Immunofluorescence staining of ACSL4 and GPx4 (scale bar = 100 μm). All experiments and images shown are representative. (For interpretation of the references to colour in this figure legend, the reader is referred to the Web version of this article.)

3.5. PAE exhibits a comparable chondrocyte-protective and anti-ferroptotic effect to ACSL4 knockdown in chondrocytes

Molecular docking confirmed the interaction between PAE and ACSL4 (Fig. 5A). Multiple groups of residues form interactions between ACSL4 and PAE. The energy associated with the binding of the protein-ligand complex was −5.7 kcal/mol, which suggests a robust interaction. Additionally, the interplay between PAE and ACSL4 was further characterized by the cellular thermal shift assay, and the data manifested that PAE significantly augmented the thermostability of ACSL4 when compared with the control (Supplementary Fig. S2A). Furthermore, the in situ binding of PAE to ACSL4 was verified through the drug affinity responsive target stability assay, a methodology employed for identifying label-free small-molecule targets based on the decrease in protease susceptibility of the target protein upon drug binding. The outcomes suggested that PAE shielded ACSL4 from degradation by pronase in chondrocytes (Supplementary Fig. S2B). To further investigate, we knocked down ACSL4 using small interfering RNA. The results showed that, compared to IL-1β, silencing ACSL4 (si-ACSL4) decreased levels of key proteins involved in ferroptosis (ACSL4 and GPx4) and ECM degradation (ADAMTS5), while enhancing the expression of chondrogenic markers (SOX9 and COL2A1) (Fig. 5B∼5D). Notably, PAE application exerted similar effects on ferroptosis, ECM degradation, and chondrogenic markers as ACSL4 knockdown, demonstrating comparable chondrocyte-protective and anti-ferroptotic effects (Fig. 5B∼5D).

3.6. PAE protects chondrocytes from the abnormal ECM metabolism generated by ACSL4 overexpression

To determine that PAE regulates chondrocytes by inhibiting ACSL4, we analyzed the effects of PAE treatment after chondrocytes overexpressed ACSL4 using an overexpression plasmid. First, the up-regulation of the expression of ACSL4 and its downstream effector (LPCAT3) confirmed successful overexpression (Supplementary Fig. S3). As shown in Supplementary Fig. S3, ACSL4 overexpression significantly suppressed cartilage anabolism and promoted cartilage catabolism. However, when PAE was added to the transfection group, it reversed the trend of ACSL4 overexpression, increased anabolism and reduced

catabolism in chondrocytes (Supplementary Fig. S3). Together with the results of the overexpression and knockdown *in vitro* experiments, these data confirmed that PAE protects chondrocytes from ferroptosis and abnormal ECM metabolism by inhibiting ACSL4.

3.7. PAE attenuates cartilage degeneration in vivo

We further investigated PAE's potential to mitigate OA progression *in vivo*. The OA mouse model was created via DMM surgery (Fig. 6A). Throughout the experiment, no animals succumbed to accidents or other unexpected causes, and no infections or inflammations were observed at the surgical sites. The safety of PAE local injection into the joint cavity appears promising, evidenced by the steady increase in body weight of mice in each group (Supplementary Fig. S4A). Additionally, historical evaluations showed no significant differences in major organs among all groups (Supplementary Fig. S4B).

Micro-computed tomography (micro-CT) analysis revealed a significant increase in osteophyte formation, including size and maturity, 8 weeks post-DMM surgery (Fig. 6B, D, and 6E) ($P < 0.05$). PAE treatment restrained osteophyte formation (Fig. 6B, D, and 6E) ($P < 0.05$). To comprehensively assess articular cartilage damage in knee joints among groups, histological analyses, including H&E, SOFG, and TB staining, were conducted. Histopathological examination of the DMM group showed progressive articular cartilage degeneration, leading to decreased cartilage thickness and increased surface roughness (Fig. 6C and H) ($P < 0.05$). Conversely, PAE treatment suppressed cartilage thickness loss and alleviated chondrocyte disorganization in mouse knee joints (Fig. 6C and H) ($P < 0.05$). Modified Mankin and Osteoarthritis Research Society International (OARSI) scores indicated that intra-articular PAE injection significantly ameliorated articular cartilage destruction (Fig. 6F and G) ($P < 0.05$). These findings indicate that PAE can decelerate articular cartilage degeneration in the mouse OA model.

3.8. PAE alleviates ECM degradation and ferroptosis in chondrocytes within the surgery-induced mouse OA model

To further investigate PAE's impact on ferroptosis in chondrocytes within the OA mouse model, immunohistochemical (IHC) analysis was conducted. IHC analysis revealed significant upregulation of ADAMTS5 and MMP3 expression in the DMM group (Fig. 7) ($P < 0.05$). Our investigation also showed elevated levels of ferroptosis-related markers, such as 4-HNE and ACSL4, and reduced GPx4 expression in the DMM group when contrasted with the Sham group (Fig. 7) ($P < 0.05$). Treatment with varying concentrations of PAE partially alleviated these changes (Fig. 7) ($P < 0.05$). Collectively, these *in vivo* findings strongly support that PAE can attenuate cartilage degradation and ferroptosis, thereby impeding OA progression in the mouse model. These results align with our *in vitro* observations.

4. Discussion

Emerging evidence suggests that lipid peroxidation-induced ferroptosis significantly contributes to cartilage degradation in OA [26]. Hence, the inhibition of lipid peroxidation and ferroptosis in chondrocytes might represent a new therapeutic approach for OA. ACSL4, plays a pivotal role in the regulation of lipid peroxidation and ferroptosis by activating polyunsaturated fatty acids and orchestrating lipid metabolism reprogramming [8,31]. Researchers have shown that inhibiting ACSL4 activity or expression is a critical intervention to prevent ferroptosis by suppressing lipid peroxidation [32,33]. Among candidate drugs, PAE, a natural product from Paeonia, has been shown to significantly inhibit ferroptosis in neuronal cells treated with heme through the inhibition of ACSL4 [18], indicating its potential as a ferroptosis inhibitor in other related diseases. In this study, we demonstrated that PAE inhibits chondrocyte ferroptosis and alleviates OA progression by targeting ACSL4.

In vitro, an inflammatory environment and iron overload were induced in chondrocyte cultures by adding IL-1β and FAC to the media. Consistent with previous findings [6,34–39], IL-1β/FAC treatment significantly promoted ECM degradation, inhibited cell proliferation, increased iron/ROS/lipid ROS levels, reduced ΔΨm, and damaged mitochondria. These changes led to increased chondrocyte death, with significant alterations in ferroptosis regulators (ACSL4, SLC7A11, and GPx4), ultimately causing ferroptosis. Following PAE intervention, intracellular iron/ROS/lipid ROS levels decreased, apoptosis was reduced, ACSL4/4-HNE expression was downregulated, and GPx4/SLC7A11 expression was upregulated. Additionally, PAE shows similar chondrocyte-protective and anti-ferroptotic effects to ACSL4 knockdown in chondrocytes. The *in vivo* study established the OA model through DMM surgery. The OA group showed accelerated cartilage degeneration, increased osteophyte formation, and higher expression of 4-HNE, ACSL4, ADAMTS5, and MMP3 compared to the Sham and DMM groups. After PAE intervention, cartilage deterioration was reduced, osteophyte formation was limited, and the elevated expression indicators were decreased, along with upregulation of GPx4. These results demonstrate that PAE is an effective ferroptosis suppressor in chondrocytes mediated by ACSL4, protecting osteoarthritic cartilage from destruction (Fig. 8).

In contrast to other well-researched types of cell death, a standardized method or biomarker for identifying ferroptosis is presently lacking [21,40]. To enhance methodological rigor, we used multiple detection methods and various evaluation indicators for ferroptosis based on previous experience. However, certain limitations must be acknowledged. OA is fundamentally a degenerative disease influenced by multiple factors and cell types [41]. This study solely examined PAE's pathogenic mechanism on ferroptosis in chondrocytes. Further research is necessary to investigate other cells (such as macrophages) and pathogenic factors. Secondly, structural and regenerative differences between mouse and human chondrocytes suggest that the findings may not directly apply to humans. Thirdly, while clinical OA progression spans years or decades, our *in vitro* intervention lasted 48 h, and the *in vivo* experiment lasted 8 weeks. Although we observed the *in vivo* biosafety of PAE, further studies are needed to evaluate its safety in treating OA. Fourthly, male C57BL/6 mice are generally acknowledged to reach sexual maturity at approximately 6 weeks of age. Several studies have utilized DMM surgery to establish OA models in these 6-week-old mice [42–46]. However, given that OA is an age-related degenerative cartilage disease, it may be more appropriate to select older C57BL/6 mice (8–12 weeks). We will make corresponding adjustments in future studies. Fifthly, in the *in vivo* experiment, we failed to inject low and high concentrations of PAE into the joint cavity of the Sham group to evaluate the effects of different concentrations of PAE on healthy knee cartilage. We will make targeted adjustments in this regard in future consecutive studies. Finally, as hormonal fluctuations between different phases of the estrous and menstrual cycles in female mice may unavoidably introduce variables in experiments and data analysis [47],

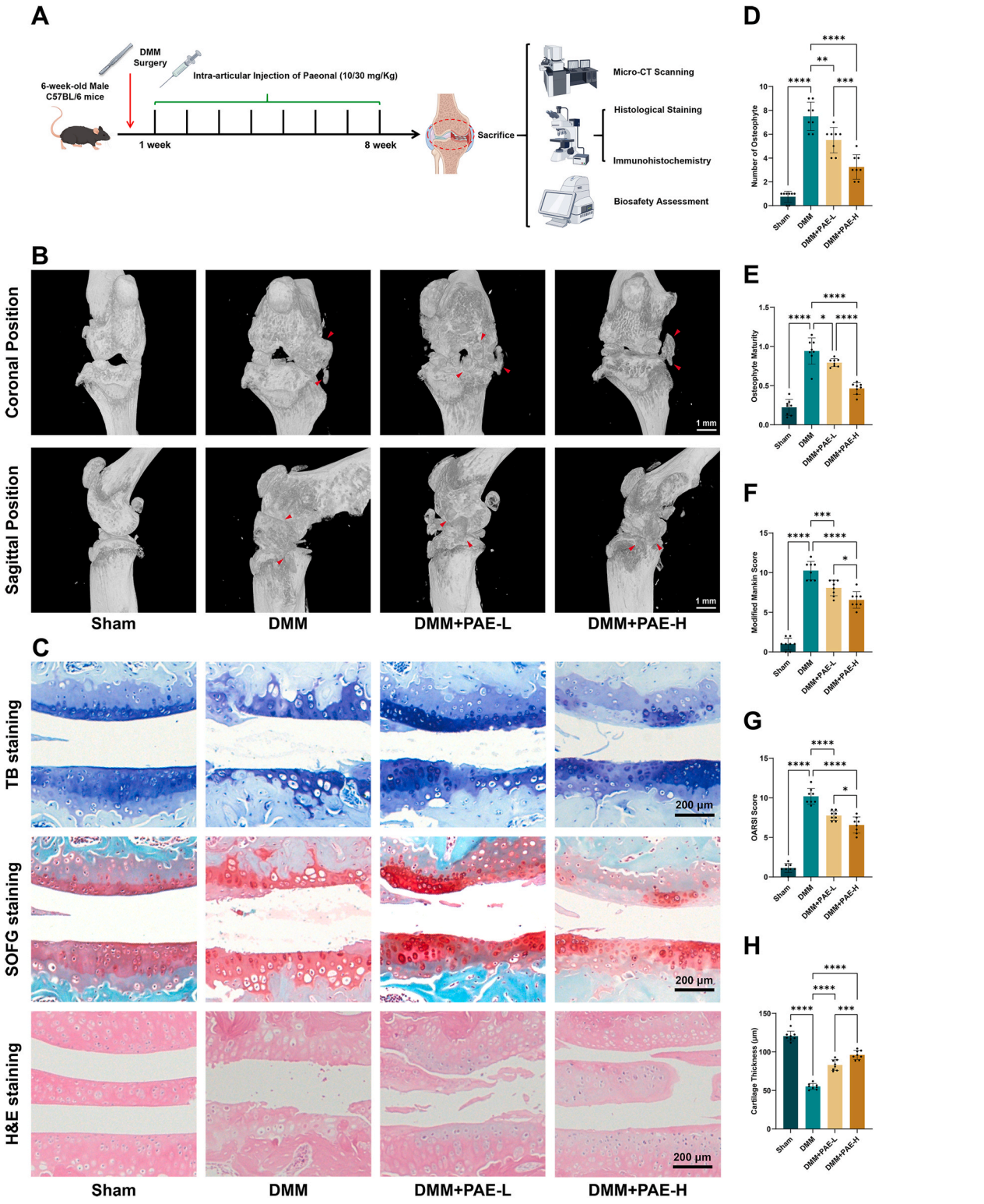

Fig. 6. PAE attenuates cartilage degeneration *in vivo*: (A) Schematic diagram of the experimental design using animals. Created using Figdraw (https://www.figdraw.com/static/index.html#/). (B) Three-dimensional coronal and sagittal images of mouse knee joints reconstructed by micro-CT, with a red arrow indicating osteophyte formation (scale bar = 1 mm). (C) Histological assessments of knee sections from each group, including TB, SOFG, and H&E staining (scale bar = 200 μm). (D) Quantification of articular osteophytes in each group (n = 8 per group). (E) Quantitative analysis of osteophyte maturity in each group (n = 8 per group). (F) Modified Mankin scores for each group (n = 8 per group). (G) OARSI scores for four groups of mice (n = 8 per group). (H) Measurement of cartilage thickness in knee joints among the four groups (n = 8 per group). Two-tailed *P* values were calculated with statistical significance defined as $P < 0.05$, denoted as 'ns' for no statistical difference, and indicated as $^{*}P < 0.05$, $^{**}P < 0.01$, $^{***}P < 0.001$. All experiments and images shown are representative. (For interpretation of the references to colour in this figure legend, the reader is referred to the Web version of this article.)

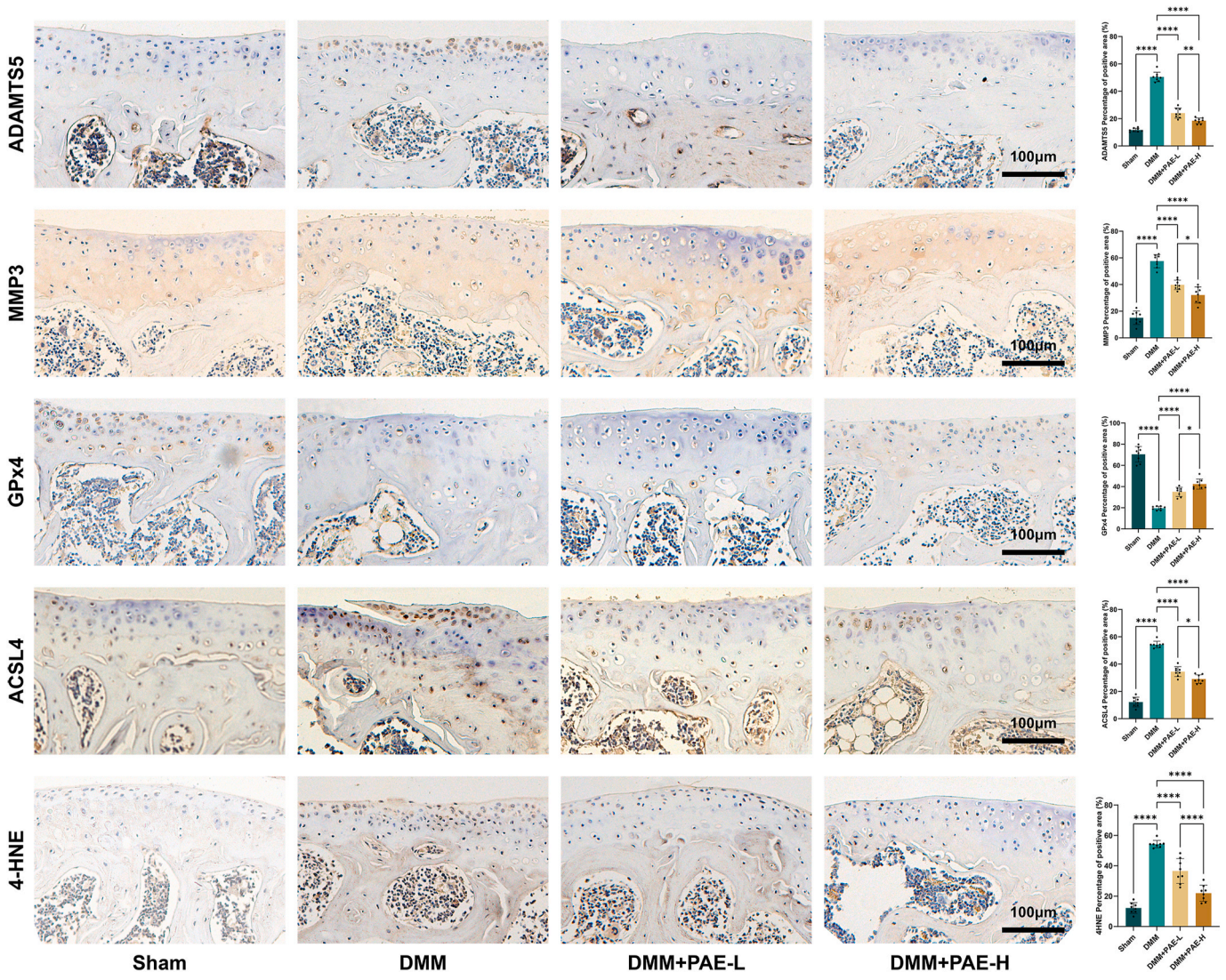

Fig. 7. PAE alleviates ECM degradation and ferroptosis in chondrocytes within the surgery-induced mouse OA model: IHC assay of ADAMTS5, MMP3, GPx4, ACSL4, and 4-HNE in articular cartilage of each group (scale bar = 100 μm), with quantification of IHC analysis for ADAMTS5, MMP3, GPx4, ACSL4, and 4-HNE (n = 8 per group). Two-tailed *P* values were calculated with statistical significance defined as $P < 0.05$, denoted as 'ns' for no statistical difference, and indicated as $^{*}P < 0.05$, $^{**}P < 0.01$, $^{***}P < 0.001$. All experiments and images shown are representative.

we employed only male mice. Nevertheless, given the statistically significant outcomes, we remain optimistic about PAE's potential for treating OA and consider it worthy of further investigation.

We are entering a new age of therapies that are specifically targeted at the molecular level. Examining the molecular foundations and pathways involved in the progression of OA, investigating molecular modulations, and creating personalized therapeutic agents are among the most promising avenues of research in OA. Given the intricacy of OA, it may be essential to focus on multiple pathways or adopt a systematic approach for effective treatment. Future studies should take into account the combined application of PAE alongside other therapeutic agents or treatments, including hormonal therapies. Despite its broad pharmacological effects, PAE's clinical application is limited by poor water solubility, rapid metabolism, and low bioavailability. Therefore, significant effort must be invested in creating novel dosage forms and enhancing their pharmacokinetics and pharmacodynamics.

5. Conclusion

This study provides the first compelling evidence that PAE effectively inhibits ferroptosis in chondrocytes by targeting ACSL4 during OA progression. This finding enriches our comprehension of PAE's pharmacological mechanism against OA and determines a novel therapeutic target, laying the groundwork for future clinical trials and emphasizing

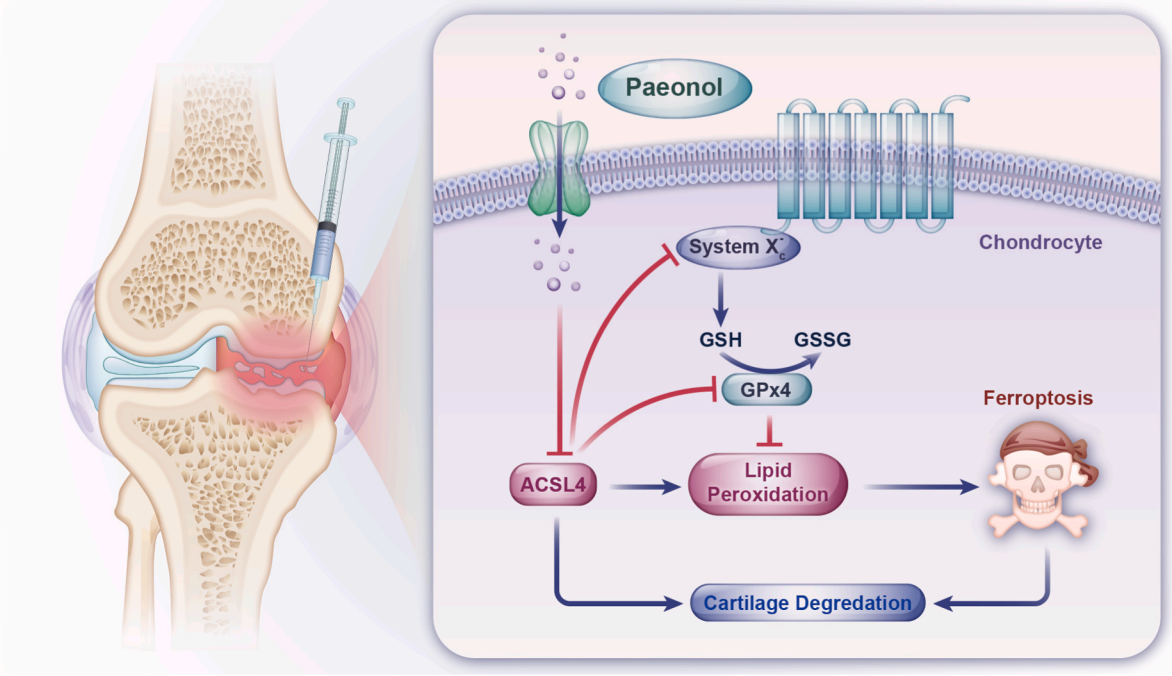

Fig. 8. Schematic illustration of the role of PAE in protecting chondrocytes from ferroptosis and attenuating OA progression by inhibiting ACSL4.

the distinctive contribution of this work to advancing OA therapy.

CRediT authorship contribution statement

Siyang Cao: Conceptualization, Investigation, Writing – original draft. **Yihao Wei:** Data curation, Visualization, Writing – review & editing, Formal analysis. **Ao Xiong:** Resources, Methodology. **Yaohang Yue:** Validation, Software, Supervision. **Jun Yang:** Resources, Methodology. **Deli Wang:** Validation, Software, Supervision. **Xiyu Liu:** Validation, Software, Supervision. **Hui Zeng:** Project administration, Funding acquisition, Resources. **Dongquan Shi:** Supervision, Writing – review & editing. **Ye Li:** Project administration, Funding acquisition, Resources.

Ethics statement

All animal procedures comply with ARRIVE guidelines, the U.K. Animals (Scientific Procedures) Act, 1986, European guidelines (2010/63/EU), and the Regulations for the Administration of Affairs Concerning Experimental Animals approved by the State Council of the People's Republic of China. The Animal Ethics Committee of the Shenzhen Peking University-Hong Kong University of Science and Technology Medical Center (No. 2023-138) approved the study.

Data availability statement

Datasets used or analyzed in this study are available from the corresponding authors upon reasonable request.

Funding

Grants for this study were provided by the National Natural Science Foundation of China (No. 82172432; No. 82302713); the Hong Kong Polytechnic University start-up Fund for RAPs (P0044120); the Large Equipment Fund(P0051081); the Guangdong Basic and Applied Basic Research Foundation (No. 2022A1515220038; No. 2021A1515220037; No. 2022B1515120046); the Shenzhen High-Level Hospital Construction Fund; the Shenzhen Key Laboratory of Orthopaedic Diseases and Biomaterials Research (ZDSYS20220606100602005); the Shenzhen Key Medical Discipline Construction Fund (No. SZXK023); the Sanming Project of Medicine in Shenzhen (No. SZSM202211038); the Research and Development Projects of Shenzhen (No. JCYJ20210324110214040; No. JCYJ20220818102815033); the Shenzhen Sustainable Development Project (No. KCXFZ20201221173411031).

Declaration of competing interest

The authors declare that they have no known competing financial interests or personal relationships that could have appeared to influence the work reported in this paper.

Acknowledgments

We thank Home for Researchers (https://www.home-for-researchers.com) for language editing assistance and the funding organizations for their support. We also acknowledge Free Science for creating the graphical abstract and Fig. 8. Fig. 6A was created using Figdraw (https://www.figdraw.com/static/index.html#/).

Appendix A. Supplementary data

Supplementary data to this article can be found online at https://doi.org/10.1016/j.jot.2024.10.005.

References

[1] Hunter D, March L, Chew M. Osteoarthritis in 2020 and beyond: a lancet commission. Lancet (London, England) 2020;396(10264):1711–2.
[2] Cao F, Xu Z, Li XX, Fu ZY, Han RY, Zhang JL, et al. Trends and cross-country inequalities in the global burden of osteoarthritis, 1990-2019: a population-based study. Ageing Res Rev 2024;99:102382 [eng].
[3] Latourte A, Kloppenburg M, Richette P. Emerging pharmaceutical therapies for osteoarthritis. Nat Rev Rheumatol 2020;16(12):673–88 [eng].
[4] Zhu R, Wang Y, Ouyang Z, Hao W, Zhou F, Lin Y, et al. Targeting regulated chondrocyte death in osteoarthritis therapy. Biochem Pharmacol 2023;215:115707 [eng].
[5] Cao S, Wei Y, Yue Y, Xiong A, Zeng H. Zooming in and out of programmed cell death in osteoarthritis: a scientometric and visualized analysis. J Inflamm Res 2024;17:2479–98 [eng].

[6] Yao X, Sun K, Yu S, Luo J, Guo J, Lin J, et al. Chondrocyte ferroptosis contribute to the progression of osteoarthritis. Journal of orthopaedic translation 2021;27:33–43.
[7] Cao S, Wei Y, Xu H, Weng J, Qi T, Yu F, et al. Crosstalk between ferroptosis and chondrocytes in osteoarthritis: a systematic review of in vivo and in vitro studies. Front Immunol 2023;14:1202436 [eng].
[8] Belavgeni A, Meyer C, Stumpf J, Hugo C, Linkermann A. Ferroptosis and necroptosis in the kidney. Cell Chem Biol 2020;27(4):448–62 [eng].
[9] Kagan VE, Mao G, Qu F, Angeli JP, Doll S, Croix CS, et al. Oxidized arachidonic and adrenic PEs navigate cells to ferroptosis. Nat Chem Biol 2017;13(1):81–90 [eng].
[10] Zhang HL, Hu BX, Li ZL, Du T, Shan JL, Ye ZP, et al. PKCβII phosphorylates ACSL4 to amplify lipid peroxidation to induce ferroptosis. Nat Cell Biol 2022;24(1):88–98 [eng].
[11] Xu Y, Yang Z, Dai T, Xue X, Xia D, Feng Z, et al. Characteristics and time points to inhibit ferroptosis in human osteoarthritis. Sci Rep 2023;13(1):21592 [eng].
[12] Xu W, Zhang B, Xi C, Qin Y, Lin X, Wang B, et al. Ferroptosis plays a role in human chondrocyte of osteoarthritis induced by IL-1β in vitro. Cartilage 2023;14(4):455–66 [eng].
[13] He W, Lin X, Chen K. Specificity protein 1-mediated ACSL4 transcription promoted the osteoarthritis progression through suppressing the ferroptosis of chondrocytes. J Orthop Surg Res 2023;18(1):188.
[14] Pitschmann A, Purevsuren S, Obmann A, Natsagdorj D, Gunbilig D, Narantuya S, et al. Traditional Mongolian Medicine: history and status quo. Phytochem Rev;12(4):943-959.
[15] Cao S, Wei Y, Yue Y, Chen Y, Liao S, Li A, et al. Targeting ferroptosis unveils a new era for traditional Chinese medicine: a scientific metrology study. Front Pharmacol 2024;15:1366852 [English].
[16] Wang Y, Li B-S, Zhang Z-H, Wang Z, Wan Y-T, Wu F-W, et al. Paeonol repurposing for cancer therapy: from mechanism to clinical translation. Biomed Pharmacother 2023;165:115277.
[17] Wu R, Liu Y, Zhang F, Dai S, Xue X, Peng C, et al. Protective mechanism of Paeonol on central nervous system. Phytother Res : PTR 2024;38(2):470–88 [eng].
[18] Jin ZL, Gao WY, Liao SJ, Yu T, Shi Q, Yu SZ, et al. Paeonol inhibits the progression of intracerebral haemorrhage by mediating the HOTAIR/UPF1/ACSL4 axis. ASN neuro 2021;13:17590914211010647 [eng].
[19] Liu C, Yi X, Yan J, Liu Q, Cao T, Liu S. Paeonol improves angiotensin II-induced cardiac hypertrophy by suppressing ferroptosis. Heliyon 2023;9(9):e19149 [eng].
[20] Liu S, Cao X, Zhang T, Zhang C, Qu J, Sun Y, et al. Paeonol ameliorates endometrial hyperplasia in mice via inhibiting PI3K/AKT pathway-related ferroptosis. Phytomedicine 2023;109:154593 [eng].
[21] Ru Q, Li Y, Xie W, Ding Y, Chen L, Xu G, et al. Fighting age-related orthopedic diseases: focusing on ferroptosis. Bone research 2023;11(1):12.
[22] Blom AB, van Lent PL, Libregts S, Holthuysen AE, van der Kraan PM, van Rooijen N, et al. Crucial role of macrophages in matrix metalloproteinase-mediated cartilage destruction during experimental osteoarthritis: involvement of matrix metalloproteinase 3. Arthritis Rheum 2007;56(1):147–57 [eng].
[23] Glasson SS, Askew R, Sheppard B, Carito B, Blanchet T, Ma HL, et al. Deletion of active ADAMTS5 prevents cartilage degradation in a murine model of osteoarthritis. Nature 2005;434(7033):644–8 [eng].
[24] Breulmann FL, Hatt LP, Schmitz B, Wehrle E, Richards RG, Della Bella E, et al. Prognostic and therapeutic potential of microRNAs for fracture healing processes and non-union fractures: a systematic review. Clin Transl Med 2023;13(1):e1161 [eng].
[25] Stockwell BR. Ferroptosis turns 10: emerging mechanisms, physiological functions, and therapeutic applications. Cell 2022;185(14):2401–21.
[26] Zhang X, Hou LA-O, Guo Z, Wang G, Xu J, Zheng Z, et al. Lipid peroxidation in osteoarthritis: focusing on 4-hydroxynonenal, malondialdehyde, and ferroptosis. Cell death discovery 2023;9(1):320 [eng].
[27] Miao Y, Chen Y, Xue F, Liu K, Zhu B, Gao J, et al. Contribution of ferroptosis and GPX4's dual functions to osteoarthritis progression. EBioMedicine 2022;76:103847.
[28] Jin L, Alesi GN, Kang S. Glutaminolysis as a target for cancer therapy. Oncogene 2016;35(28):3619–25 [eng].
[29] Gaschler MM, Andia AA, Liu H, Csuka JM, Hurlocker B, Vaiana CA, et al. FINO(2) initiates ferroptosis through GPX4 inactivation and iron oxidation. Nat Chem Biol 2018;14(5):507–15 [eng].
[30] Gao M, Yi J, Zhu J, Minikes AM, Monian P, Thompson CB, et al. Role of mitochondria in ferroptosis. Molecular cell 2019;73(2):354. 63.e3. [eng].
[31] Dai Y, Chen Y, Mo D, Jin R, Huang Y, Zhang L, et al. Inhibition of ACSL4 ameliorates tubular ferroptotic cell death and protects against fibrotic kidney disease. Commun Biol 2023;6(1):907 [eng].
[32] Chen F, Kang R, Liu J, Tang D. The ACSL4 network regulates cell death and autophagy in diseases. Biology 2023;12(6) [eng].
[33] Ding K, Liu C, Li L, Yang M, Jiang N, Luo S, et al. Acyl-CoA synthase ACSL4: an essential target in ferroptosis and fatty acid metabolism. Chinese medical journal 2023;136(21):2521–37 [eng].
[34] Jing X, Lin J, Du T, Jiang Z, Li T, Wang G, et al. Iron overload is associated with accelerated progression of osteoarthritis: the role of DMT1 mediated iron homeostasis. Front Cell Dev Biol 2021;8:594509.
[35] Jing X, Du T, Li T, Yang X, Wang G, Liu X, et al. The detrimental effect of iron on OA chondrocytes: importance of pro-inflammatory cytokines induced iron influx and oxidative stress. J Cell Mol Med 2021;25(12):5671–80.
[36] Li S, He Q, Chen B, Zeng J, Dou X, Pan Z, et al. Cardamonin protects against iron overload induced arthritis by attenuating ROS production and NLRP3 inflammasome activation via the SIRT1/p38MAPK signaling pathway. Sci Rep 2023;13(1):13744 [eng].
[37] Jing X, Wang Q, Du T, Zhang W, Liu X, Liu Q, et al. Calcium chelator BAPTA-AM protects against iron overload-induced chondrocyte mitochondrial dysfunction and cartilage degeneration. Int J Mol Med 2021;48(4).
[38] He Q, Yang J, Pan Z, Zhang G, Chen B, Li S, et al. Biochanin A protects against iron overload associated knee osteoarthritis via regulating iron levels and NRF2/System xc-/GPX4 axis. Biomedicine & pharmacotherapy = Biomedecine & pharmacotherapie 2023;157:113915.
[39] Pan Z, He Q, Zeng J, Li S, Li M, Chen B, et al. Naringenin protects against iron overload-induced osteoarthritis by suppressing oxidative stress. Phytomedicine: international journal of phytotherapy and phytopharmacology 2022;105:154330.
[40] Wang X, Zhou Y, Min J, Wang F. Zooming in and out of ferroptosis in human disease. Front Med 2023;17(2):173–206.
[41] Zhang W, Ouyang H, Dass C, Xu J. Current research on pharmacologic and regenerative therapies for osteoarthritis. Bone research 2016;4:15040.
[42] Malaise O, Tachikart Y, Constantinides M, Mumme M, Ferreira-Lopez R, Noack S, et al. Mesenchymal stem cell senescence alleviates their intrinsic and seno-suppressive paracrine properties contributing to osteoarthritis development. Aging 2019;11(20):9128–46 [eng].
[43] Saitou T, Kiyomatsu H, Imamura T. Quantitative morphometry for osteochondral tissues using second harmonic generation microscopy and image texture information. Sci Rep 2018;8(1):2826 [eng].
[44] Niebler S, Schubert T, Hunziker EB, Bosserhoff AK. Activating enhancer binding protein 2 epsilon (AP-2ε)-deficient mice exhibit increased matrix metalloproteinase 13 expression and progressive osteoarthritis development. Arthritis Res Ther 2015;17(1):119 [eng].
[45] Schmid R, Schiffner S, Opolka A, Grässel S, Schubert T, Moser M, et al. Enhanced cartilage regeneration in MIA/CD-RAP deficient mice. Cell Death Dis 2010;1(11):e97 [eng].
[46] Hu Y, Cui J, Liu H, Wang S, Zhou Q, Zhang H, et al. Single-cell RNA-sequencing analysis reveals the molecular mechanism of subchondral bone cell heterogeneity in the development of osteoarthritis. RMD Open 2022;8(2).
[47] Sechzer JA, Rabinowitz VC, Denmark FL, McGinn MF, Weeks BM, Wilkens CL. Sex and gender bias in animal research and in clinical studies of cancer, cardiovascular disease, and depression. Ann N Y Acad Sci 1994;736:21–48 [eng].